Supporting Information

A new and highly robust light-responsive Azo-UiO-66 for highly selective and low energy post-combustion CO_2 capture and its application in a mixed matrix membrane for CO_2/N_2 separation

*Nicholaus Prasetya, Bogdan C. Donose and Bradley P. Ladewig**

Supplementary information for Figure 1 (a), (b) and (c) in the main manuscript.
These figures are created by using CrystalMaker Software. We call this a hypothetical visualization since we assume that the azobenzene group that protrudes into the pores is randomly oriented. The CrystalMaker Software itself allows us to do structure relaxation. However, the complexity of the structure hinders us to do so. Therefore, we created the graph without structural relaxation and thus call them a hypothetical visualization.

The chemical structure of the ligand is shown in Figure S 1. The purity of the ligand was confirmed by ^{1}H-NMR spectrum which is shown in Figure S 2. Upon 4 hour exposure of the free ligand under UV light, as can be seen from Figure S 3 some new peaks and peak splitting in some area also appeared confirming the isomerization process.

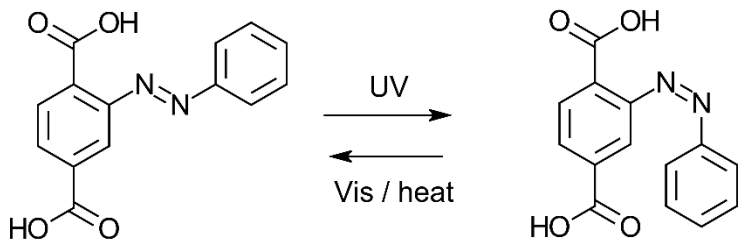

Figure S 1. Chemical structure of 2-phenyldiazenyl terephthalic acid

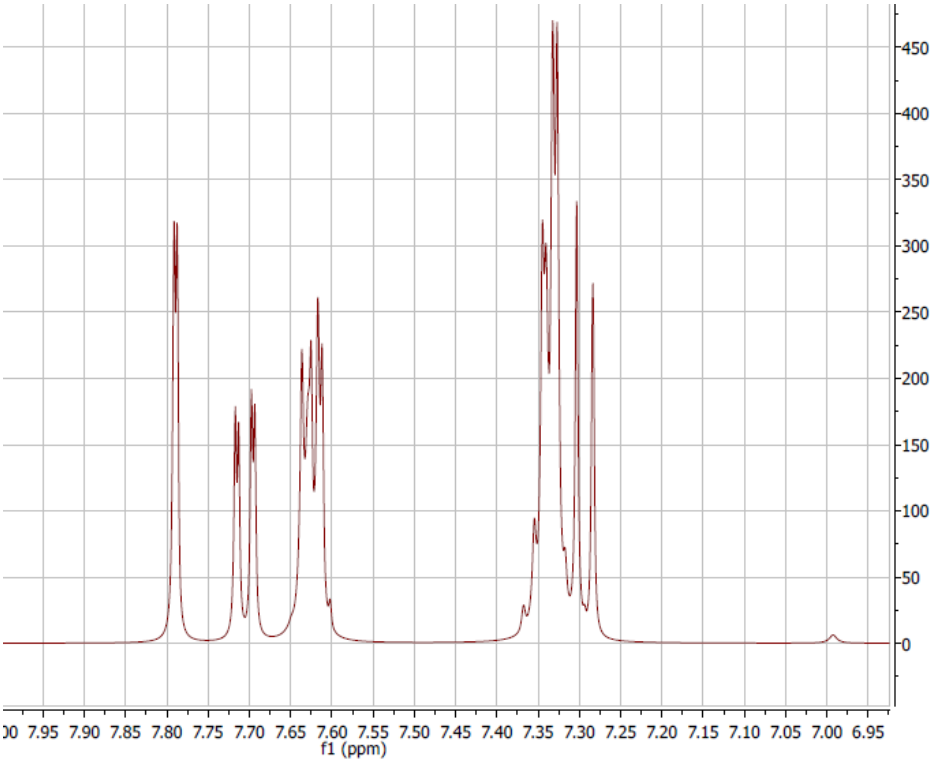

Figure S 2. ^{1}H-NMR spectrum of the free ligand (L1)

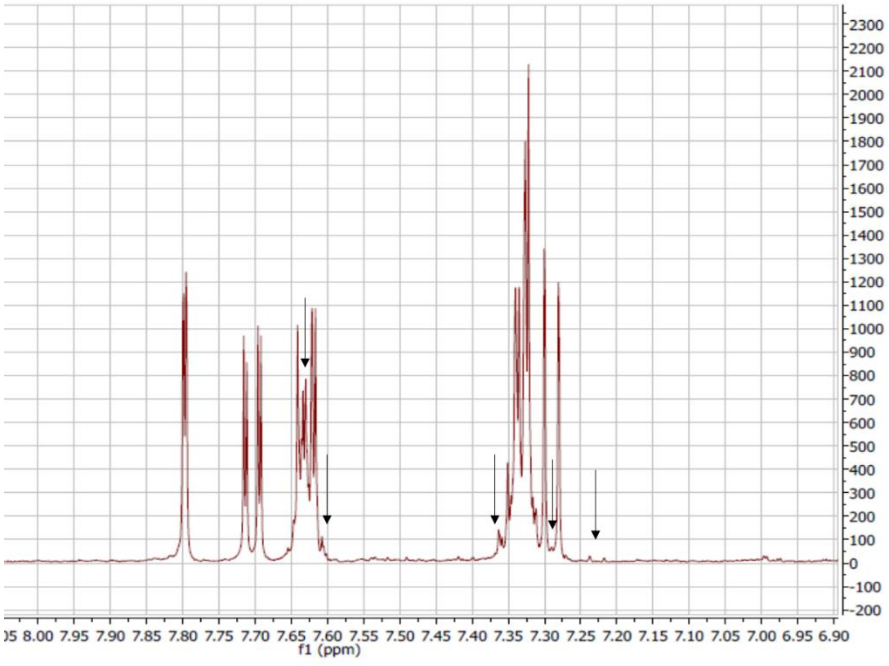

Figure S 3. ^{1}H NMR spectrum of the free ligand (L1) after 4 hour UV irradiation. Arrows indicate the appearance of new peaks and peak splitting

It was observed that negligible change of CO_2 adsorption of azo-UiO-66 occurred after ex-situ UV irradiation as can be seen in Figure S 4 The CO_2 adsorption capacity of azo-UiO-66 after ex-situ UV irradiation was found to be always similar with its non-irradiated condition.

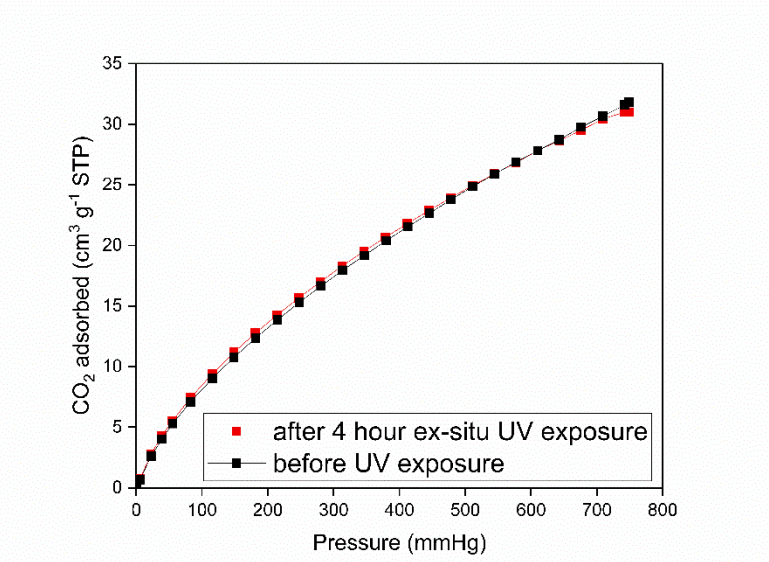

Figure S 4. CO_2 adsorption of azo-UiO-66 in pristine and after ex-situ UV exposure at 273 K

Additional SEM micrographs for the particles used in this study

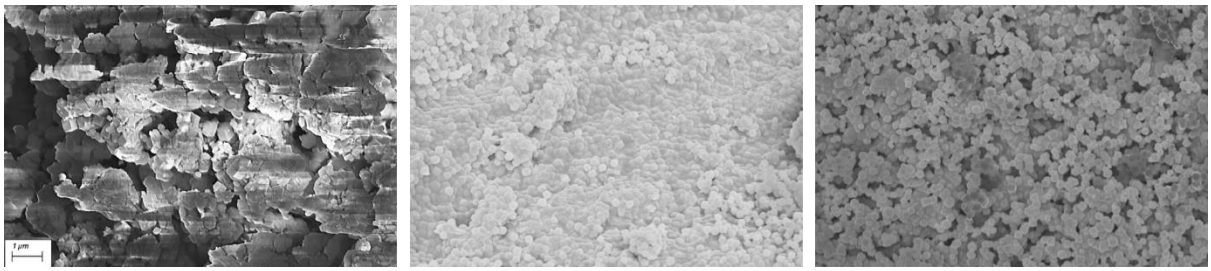

Figure S 5. From left to right: ZIF-8 from BASF, UiO-66 and Azo-UiO-66 used in this study

Two different control experiments were conducted during the CO_2 dynamic photoswitching observation. It could be seen from Figure S 6 that both ZIF-8 and UiO-66 did not exhibit any photoswitching behaviour. Lower CO_2 uptake was likely caused by temperature increase during UV light exposure

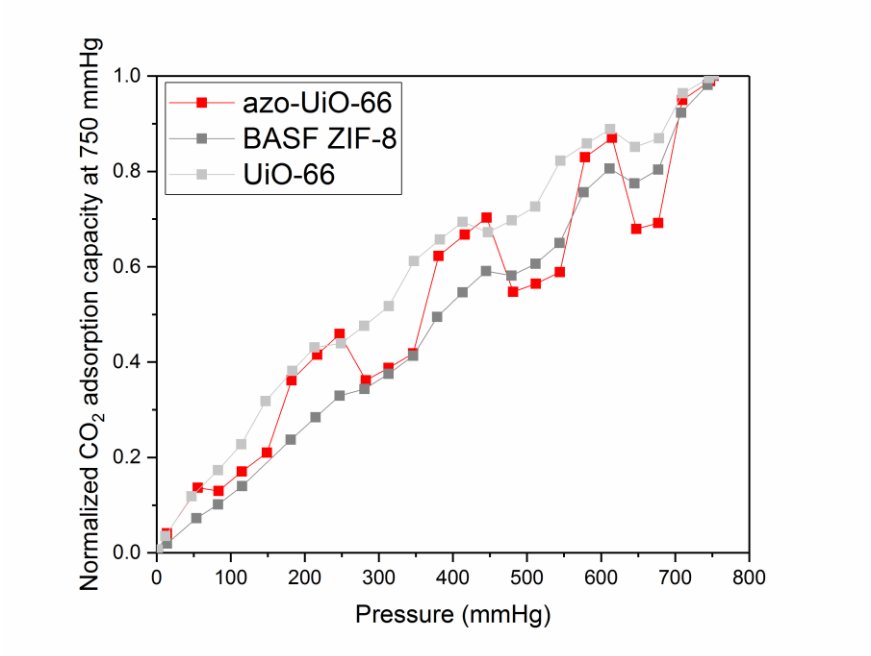

Figure S 6. CO_2 dynamic photoswitching control experiment

FTIR spectrum of the azo-UiO-66 before and immediately after UV exposure. Almost no significant difference could be observed as can be seen in Figure S 7.

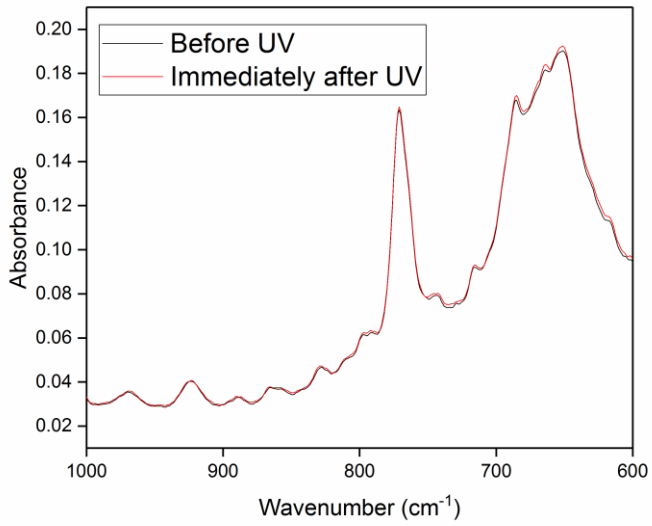

Figure S 7. FTIR spectrum of the azo-UiO-66 before and immediately after UV light irradiation

It could be seen from Figure S 8 and Figure S 9 that the ^{1}H-NMR spectrum of the digested azo-UiO-66 for non-irradiated and after-UV irradiation condition did not show any significant difference and thus not confirming any isomerization process.

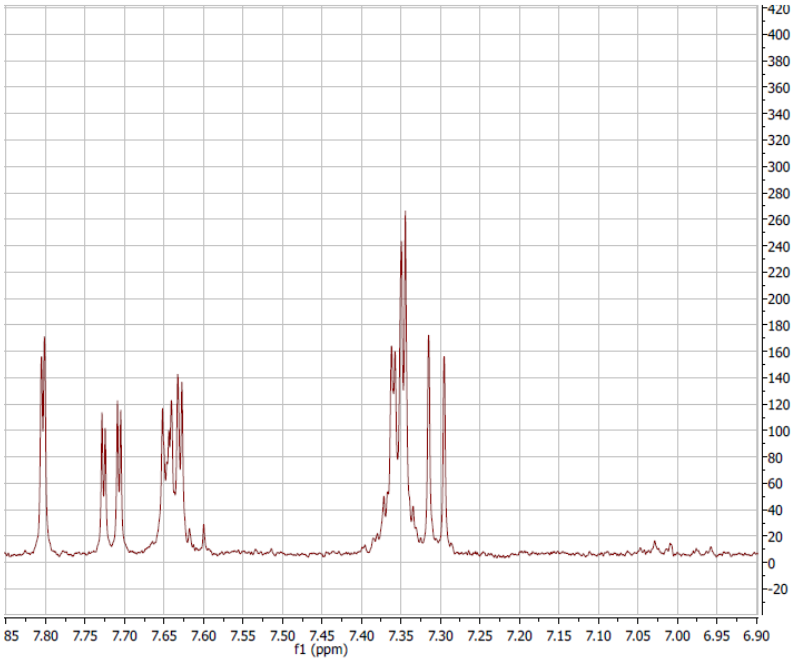

Figure S 8. ^{1}H NMR spectrum of digested azo-UiO-66

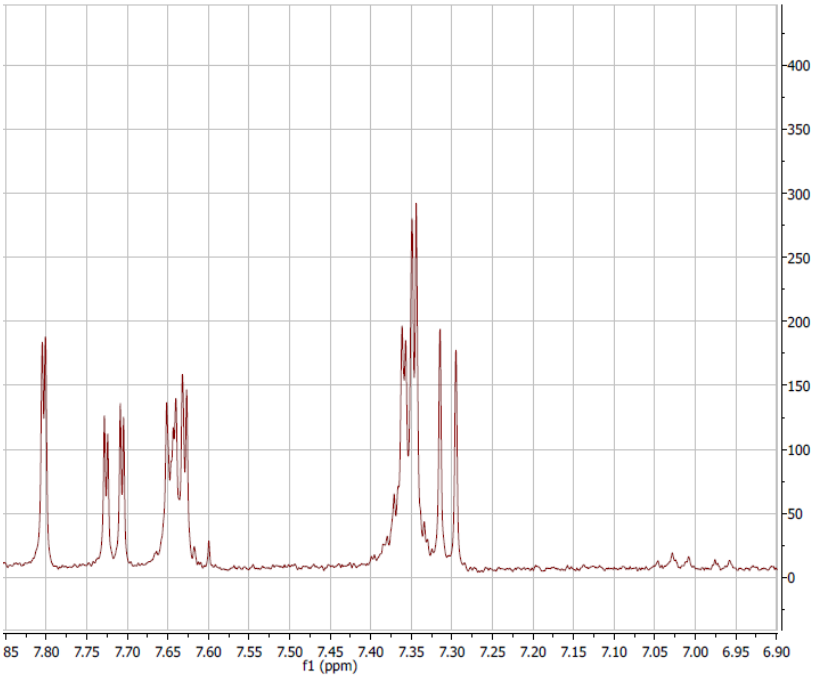

Figure S 9. ^{1}H NMR spectrum of digested azo-UiO-66 after 4 hour UV irradiation

This condition was further confirmed using UV-Vis spectroscopy as can be seen in Figure S 10. Digested azo-UiO-66 sample has a peak maxima at 316 and 423 nm corresponding to the azobenzene ligand. Although we could barely observed any significant change in the absorption region at 423 nm, we could observe a significant change at 316 nm region that

could also be related with the isomerization of azobenzene. If the azo-UiO-66 was digested first and followed by UV irradiation, the peak at 316 significantly decrease. Meanwhile if it was irradiated first and followed by digestion, almost no change was observed on the absorption at 316 nm. This indicates the ligand could be isomerized once the sample was digested but not in its solid state condition. Note that all experiments were conducted using the same concentration of samples.

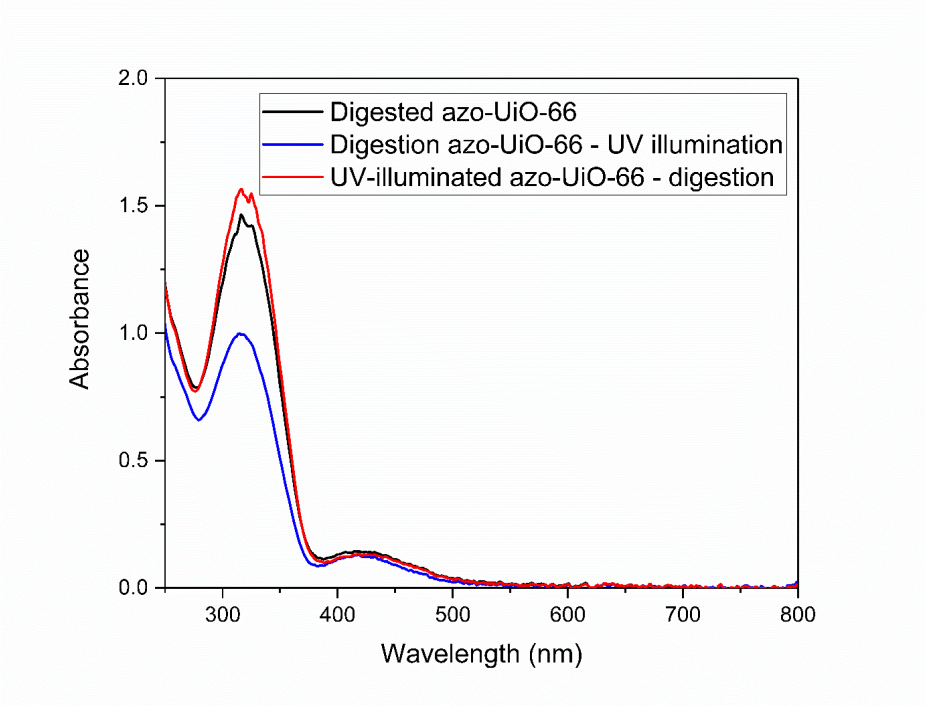

Figure S 10. UV-Vis spectrum of digested azo-UiO-66 with different sequence treatments

Various characterizations were employed for azo-UiO-66-Matrimid mixed matrix membranes to confirm the presence of the particles inside the Matrimid matrix. Figure S 11, Figure S 12 and Figure S 13 show the PXRD, FTIR-Raman and TGA-DSC results, respectively.

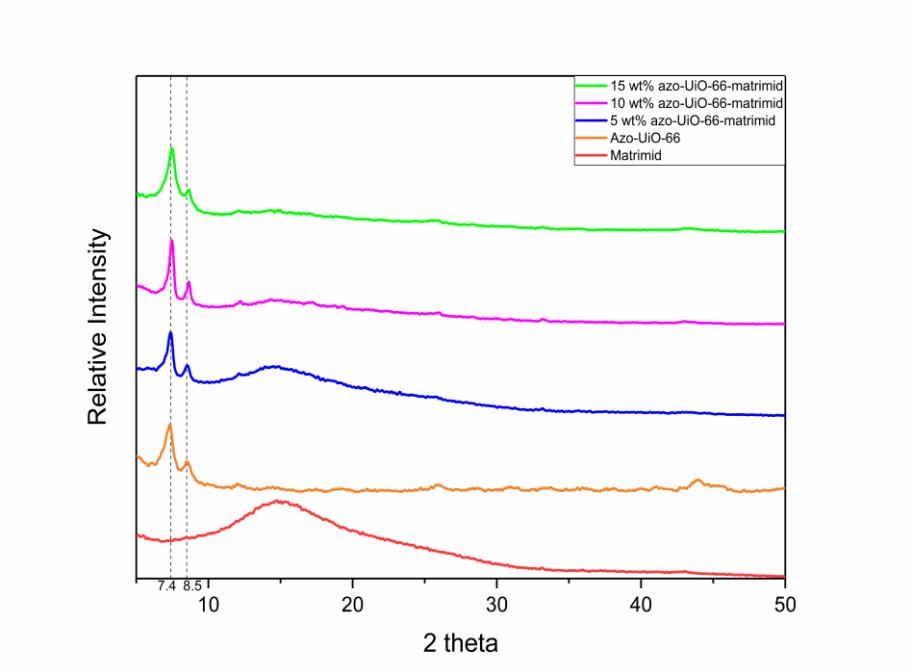

Figure S 11. PXRD patterns of the azo-UiO-66-Matrimid mixed matrix membranes

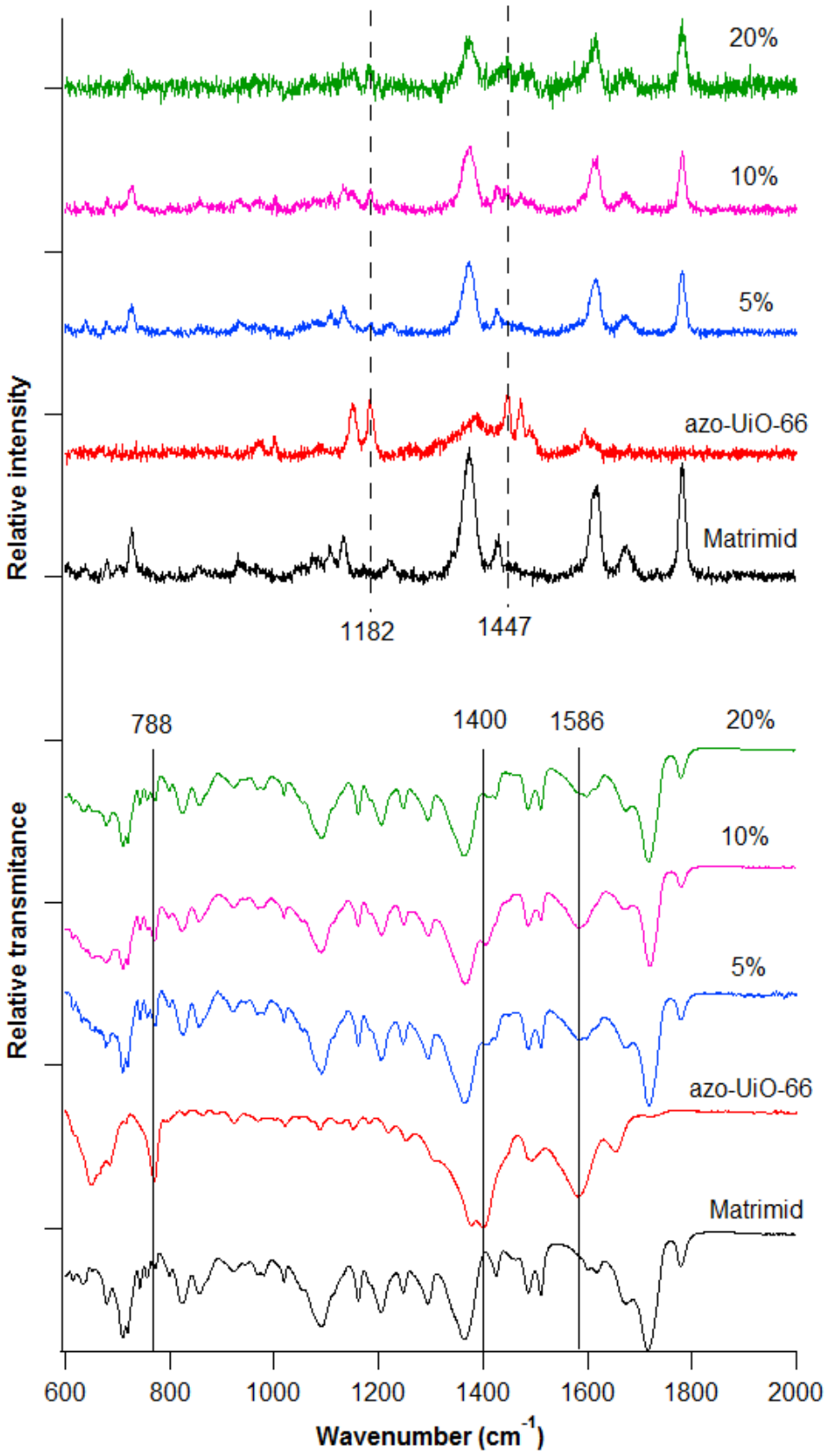

Figure S 12. FTIR and Raman spectra of azo-UiO-66-Matrimid mixed matrix membranes

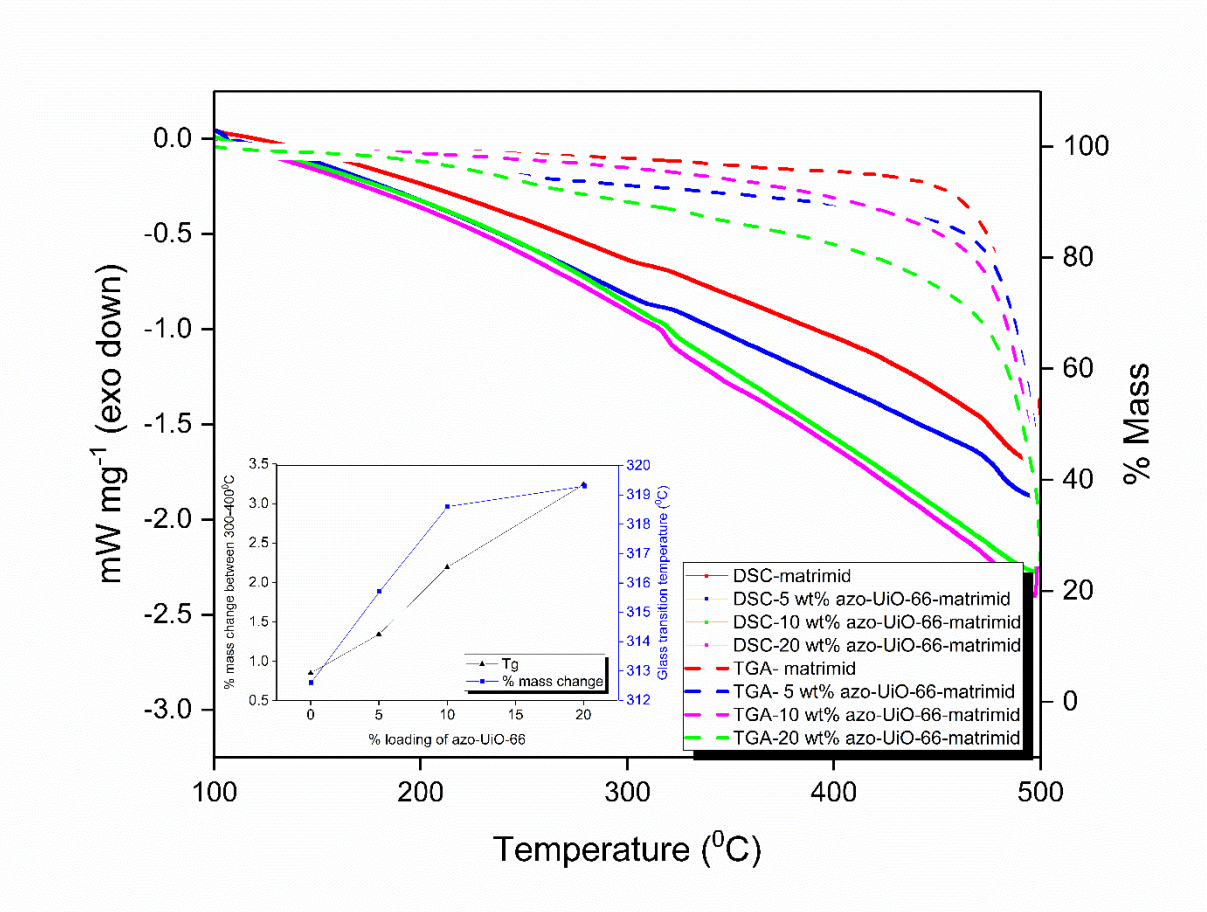

Figure S 13. TGA and DSC curve of the azo-UiO-66-Matrimid mixed matrix membranes. Inset: evaluation on the mass change and T_g of the membranes

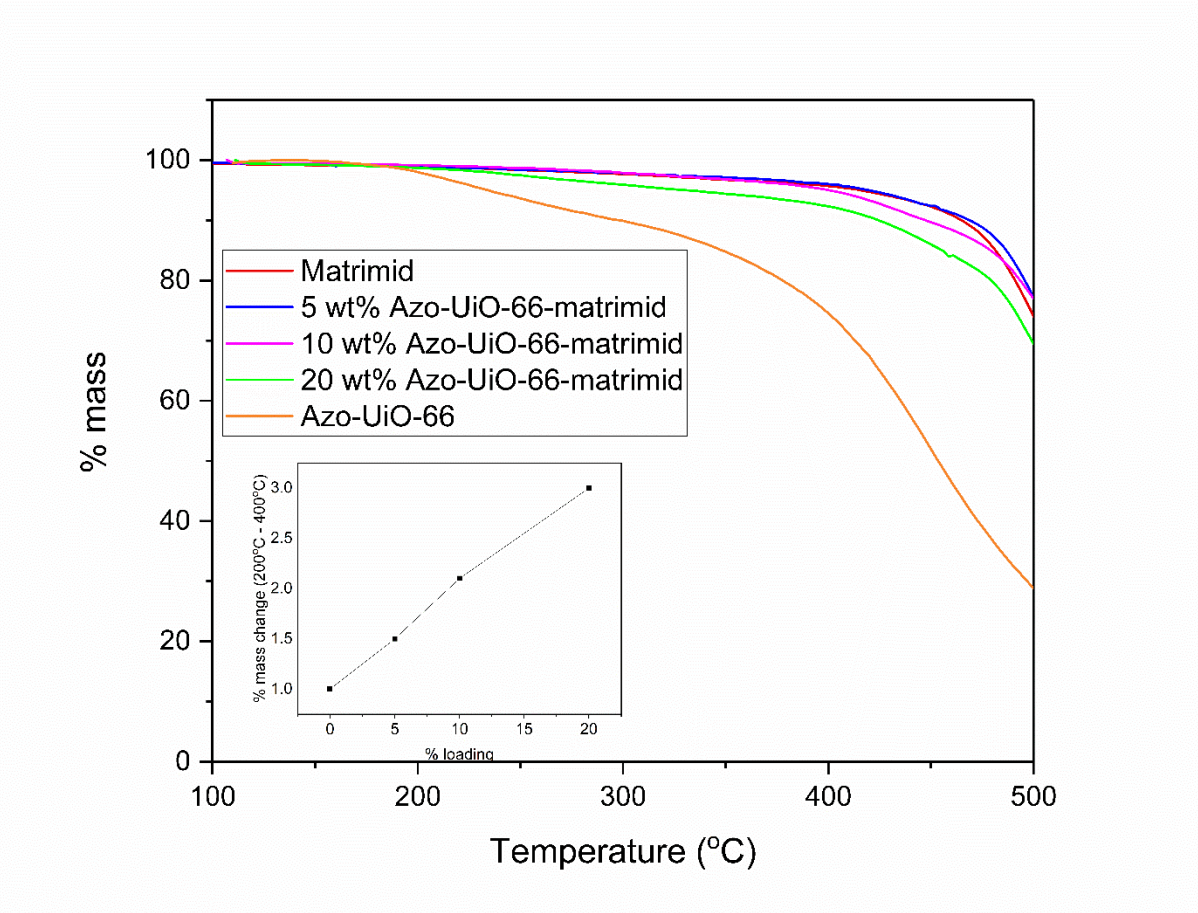

Figure S 14. TGA analysis of the mixed matrix membranes in the air atmosphere. Inset: mass change between 200°C and 400°C)

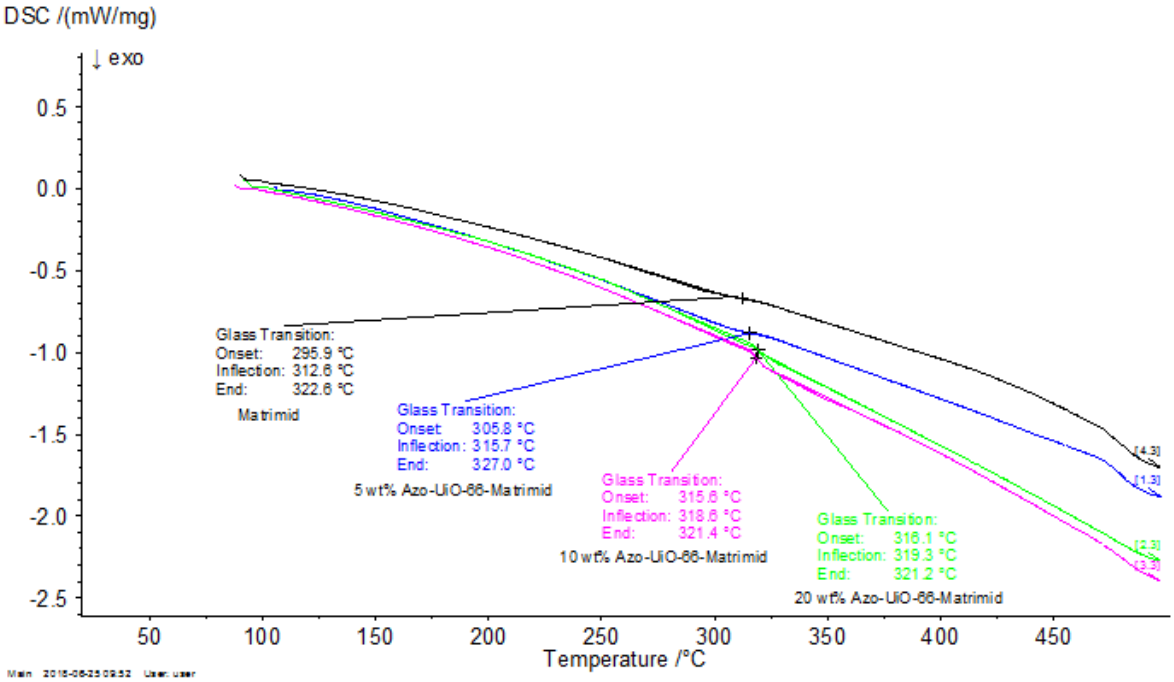

Figure S 15. DSC Analysis from Proteus Analysis Software

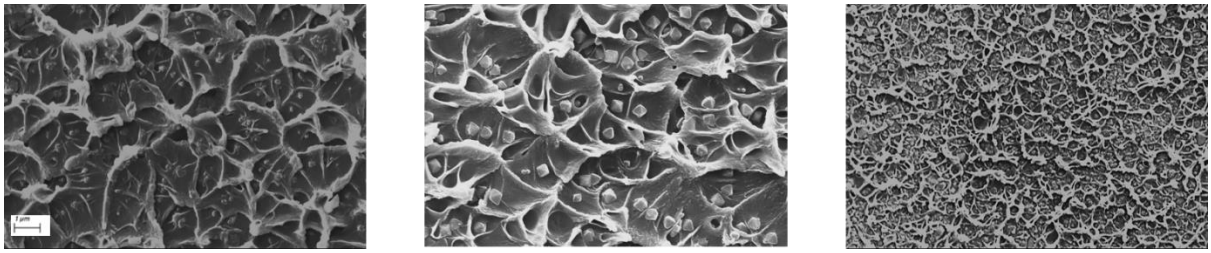

Figure S 16. Additional SEM micrographs of the MMMs cross section (left to right: 5 wt%, 10 wt% and 20 wt% Azo-UiO-66-Matrimid)

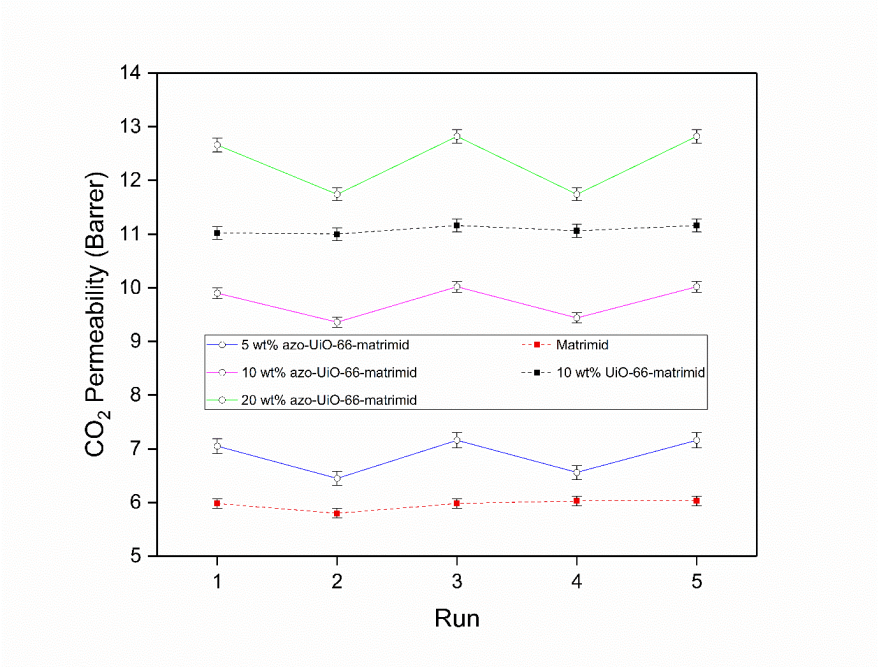

Figure S 17. CO_2 switching permeability testing of the mixed matrix membranes

Table S 1. Summary of the performance of MOF-Matrimid mixed matrix membranes for CO_2/N_2 separation

Filler	Polymer	Loading (wt%)	Permeability (Barrer)		CO_2/N_2 ideal selectivity	T (°C)	feed pressure (bar)	Ref
			CO_2	N_2				
NH_2-UiO-66	Matrimid 5218	0	8	0.28	29	25	Not stated	1
		23	23	0.66	35			
NH_2-UiO-67-PA		23	28	0.78	36			
NH_2-UiO-68-C10		23	22	0.81	27			
NH_2-UiO-69-SA		23	19	0.63	30			
MOF-5	Matrimid 5218	0	9	0.25	36	35	2	2
		10	11.1	0.28	39.64			
		20	13.8	0.4	34.5			
		30	20.2	0.52	38.85			
MCM-41	Matrimid 5218	0	6		27	25	10 bar	3
		10	7		27			
		20	8		27			
		30	10		26			
SO_3H-MCM 41	Matrimid	0	6		27			3
		10	6		30			
		20	8		30			
		30	10		31			
Cu_MOF	Matrimid	0	7.33	0.24	30.54	35	2.67	4
		9	20.54	0.66	31.12			
		17	38.27	1.33	28.77			
		23	74.08	3.44	21.53			
		29	233.9	19.89	11.76			
		33	465	102.3	4.55			
		45	3130	1204	2.6			
MOP-18	Matrimid	0	7.3	0.24	30.42	35	2.67	4
		23	9.4	0.34	27.65			
		33	14	0.61	22.95			
		45	15.6	0.6	26			
Cu-BPY-HFS	Matrimid	0	7.29	0.22	33.14	35	Not stated	5
		10	7.81	0.24	32.54			
		20	9.88	0.31	31.87			
		20	10.02	0.32	31.31			
		30	10.36	0.31	33.42			
		40	15.06	0.49	30.73			
ZIF-8	Matrimid	0	8	0.3	26.67	35		4
		20	9	0.3	30			
		30	13	0.53	24.53			
		40	25	1.05	23.81			
		50	4	0.18	22.22			

		60	7	0.44	15.91			
UiO-66	Matrimid 5218	0	6.9	0.23	29.83	35	4	This work
		10	7.8	0.26	29.4			
Azo-UiO-66		5	7.1	0.19	35			
		10	10	0.26	37			
		20	13	0.3	40			

Supplementary references

1. S. R. Venna, M. Lartey, T. Li, A. Spore, S. Kumar, H. B. Nulwala, D. R. Luebke, N. L. Rosi and E. Albenze, *Journal of Materials Chemistry A*, 2015, **3**, 5014-5022.
2. E. V. Perez, K. J. Balkus, J. P. Ferraris and I. H. Musselman, *Journal of Membrane Science*, 2009, **328**, 165-173.
3. A. L. Khan, C. Klaysom, A. Gahlaut, A. U. Khan and I. F. Vankelecom, *Journal of membrane science*, 2013, **447**, 73-79.
4. I. Musselman, K. Balkus Jr and J. Ferraris, *Mixed-Matric Membranes for CO2 and H2 Gas Separations Using Metal-Organic Framework and Mesoporus Hybrid Silicas*, University Of Texas At Dallas, 2009.
5. Y. Zhang, I. H. Musselman, J. P. Ferraris and K. J. Balkus, *Journal of Membrane Science*, 2008, **313**, 170-181.